Dyes and Pigments 125 (2016) 80–88

Contents lists available at ScienceDirect

Dyes and Pigments

journal homepage: www.elsevier.com/locate/dyepig

Solvent dependent photophysical properties and near-infrared solid-state excited state intramolecular proton transfer (ESIPT) fluorescence of 2,4,6-trisbenzothiazolylphenol

Xuan Zhang*, Jing-Yun Liu

College of Chemistry, Chemical Engineering & Biotechnology, National Engineering Research Center for Dyeing and Finishing of Textiles, Donghua University, Shanghai 201620, China

ARTICLE INFO

Article history:
Received 27 August 2015
Accepted 5 October 2015
Available online 23 October 2015

Keywords:
Benzothiazole
Excited-state intramolecular proton transfer
Near-infrared fluorescence emission
Solvent effect
Ratiometric
Anion sensing

ABSTRACT

A new excited-state intramolecular proton transfer (ESIPT) fluorophore, 2,4,6-trisbenzothiazolylphenol (**4**), was synthesized and its photophysical properties were studied with steady state absorption and emission spectroscopy as well as time-dependent density functional theory calculation. It was found that **4** showed solvent dependent absorption and fluorescence emission. In the nonpolar solvents, ESIPT occurred and only keto tautomer emission at 570 nm was observed, whereas an emission at 510 nm from the deprotonated anion species was observed in polar solvents. With addition of fluoride, the keto emission was quenched, whereas the anion emission was drastically enhanced, making a ratiometric fluorescence sensing of fluoride achievable. In solid state, **4** showed a fluorescence emission at 605 nm, which is longer than those of 2,4-dibenzothiazolylphenol (575 nm) and 4-methyl-2,6-dibenzothiazolylphenol (592 nm) respectively. Thus, the color tuning of solid state ESIPT emission were achieved from green to yellow and near-infrared by extending of the π-conjugation.

1. Introduction

Excited-state intramolecular proton transfer (ESIPT) has received considerable attention due to its importance on fundamental reaction process and promising applications on organic optoelectronic materials as well as fluorescence sensing [1–20]. In this regard, several ESIPT prototype chromophores, for example, methyl salicylate (MS) [21,22], 3-hydroxyflavone (3HF) [23,24], 2-(2′-hydroxyphenyl)benzoxazole (HBO) [25,26], and 2-(2-hydroxyphenyl) benzothiazole (HBT) [27–31], have been extensively investigated on both fundamental photophysics and potential application on luminescent materials. However, it is still a challenge to design new ESIPT fluorophores with predetermined photophysical properties. One popular strategy used for design of new fluorophores is to extending the π-conjugation [3]. HBT (**1**, Fig. 1) is the well-known ESIPT dye that usually showed both a blue emission and a green emission from enol and keto tautomers respectively [27,28]. Recently, bis-HBT derivatives 2,4-dibenzothiazolylphenol (**2**, Fig. 1), 6-dibenzothiazolylphenol (**3**, Fig. 1) have been reported to show a yellow ESIPT fluorescence emission in $CHCl_3$ solution (ca. 560 nm), which is red-shifted about 45 nm compared to the green emission (515 nm) of **1** [32]. It is therefore interesting to try for further extending of the π-conjugation by introducing the third benzothiazole group to investigate the substituent effect on ESIPT fluorescence emission of HBT derivatives. The aim of this study was to synthesize exemplary tris-HBT derivative 2,4,6-trisbenzothiazolylphenol (**4**) and investigate its photophysical properties, in comparison with those of HBT **1** and bis-HBT **2** and **3**. The tris-HBT **4** exhibits a high efficient near-infrared (NIR) solid state ESIPT emission around 605 nm with a fluorescence quantum yield of 30%,which is longer than those of HBT **1** (525 nm), bis-HBT **2** (575 nm) and **3** (592 nm) respectively. Thus, the ESIPT emission color tuning of HBT chromophore from green to yellow and red was achieved by properly extending the π-conjugation. The photophysical properties of the tris-HBT **4** were studied in detail with steady state spectroscopy and DFT/TDDFT computations, and its ratiometric sensing property for fluoride anion as well as creation of white emission was also investigated. These findings will contribute to develop highly emissive NIR fluorescent materials and ratiometric fluorescent probes based on the ESIPT chromophores.

---

* Corresponding author.
E-mail address: xzhang@dhu.edu.cn (X. Zhang).

http://dx.doi.org/10.1016/j.dyepig.2015.10.002

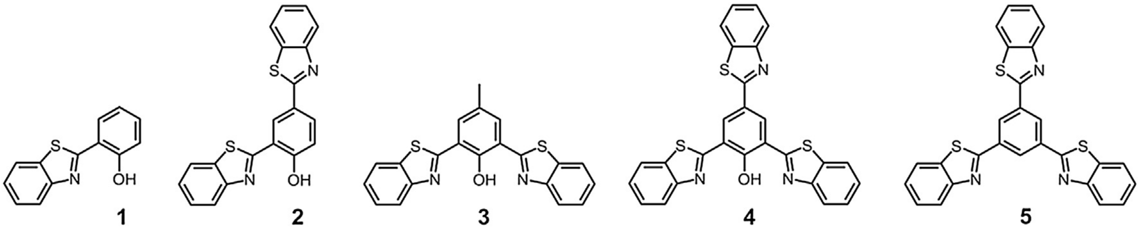

Fig. 1. Molecular structures of **1**–**5** investigated in this work.

2. Experimental section

2.1. Materials and measurements

All the chemicals are analytical grade (Sinopharm Chemical Reagents Co.) and were used as received. Fluorescence and absorption spectra were measured on a Hitachi F-7000 (Ex/Em slit widths: 2.5 nm) and a Persee TU-1901 spectrometer with a 1 cm quartz cuvette, respectively. The fluorescence quantum yield in solution was determined by using quinine sulfate ($\Phi_f = 0.546$ in 0.1 M H_2SO_4) as a standard [33]. The solid fluorescence spectra and absolute quantum yields were obtained on Edinburgh FS5 spectrofluorometer equipped with an integrating sphere (EI-FS5-SC-30). Fluorescence micrographs were recorded on Nikon ECLIPSE 80i microscope. ^{1}H NMR and ^{13}C NMR spectra were recorded on a Bruker AVANCE III 400 MHz spectrometer with TMS as standard. Mass spectra were collected on AB Sciex MALDI-TOF/TOF^{TM} MS spectrometer. Elemental analysis data were obtained on Elmentar Vario EL III system.

2.2. Synthesis

2.2.1. 2-(2-Hydroxyphenyl)benzothiazole (*1*)

1 was prepared from salicylic acid and 2-aminothiophenol according to the similarly reported procedure with some modifications [34]. Briefly, under N_2 atmosphere, salicylic acid (5 mmol) and 2-aminothiophenol (5 mmol) were dissolved in polyphosphoric acid (8 mL) and heated at 180 °C for 5 h. The mixture was cooled to room temperature and poured into 80 mL ice water. The obtained solid product was further purified by column chromatography (silica gel, hexane/dichloromethane = 10:1 v/v) to give **1** as white solid. Yield: 34.7%. ^{1}H NMR (400 MHz, $CDCl_3$), δ (*ppm*): 12.42 (s, 1H), 8.03 (d, J = 8 Hz, 1H), 7.94 (d, J = 8 Hz, 1H), 7.74 (d, J = 8 Hz, 1H), 7.55 (t, J = 10 Hz, 1H), 7.43 (m, 2H), 7.14 (d, J = 8 Hz, 1H), 6.98 (t, J = 8 Hz, 1H); ^{13}C NMR (100 MHz, $CDCl_3$), δ (*ppm*): 169.38, 157.95, 151.76, 132.79, 132.59, 128.42, 125.56, 122.16, 121.52, 119.53, 117.89, 116.77, 29.72. MALDI-TOF-MS: *m*/*z* calcd for $C_{13}H_9NOS$, 227.04; found, 228.09 $(M + H)^+$.

2.2.2. 2,4-Dibenzothiazolylphenol (*2*)

2 was prepared as previously described with some modifications [32]. Briefly, under an N_2 atmosphere, 5-formylsalicylic acid (5 mmol) and 2-aminobenzenethiol (10 mmol) were dissolved in DMSO (2 mL) and heated at 180 °C for 2 h. After cooling to room temperature, the mixture was poured into water and the crude product was collected by filtration. The obtained solid product was further purified by column chromatography (silica gel, hexane/dichloromethane = 1:1 v/v) to give **2** as pale yellow solid. Yield: 19.9%. ^{1}H NMR (400 MHz, $CDCl_3$), δ (ppm): 13.08 (s, 1H), 8.51 (s, 1H), 8.07 (d, J = 8 Hz, 1H), 8.02 (m, 1H), 7.96 (d, J = 8 Hz, 1H), 7.92 (d, J = 8 Hz, 1H), 7.47 (m, 5H), 7.23 (d, J = 12 Hz, 1H); ^{13}C NMR (100 MHz, $CDCl_3$), δ (ppm): 168.64, 166.91, 160.36, 153.89, 151.57, 134.72, 132.75, 131.90, 127.50, 126.89, 126.44, 125.91, 125.34, 125.09, 122.89, 122.31, 121.67, 121.59, 118.64, 117.21. MALDI-TOF-MS: *m*/*z* calcd for $C_{20}H_{12}N_2OS_2$, 360.04; found 361.10 $(M + H)^+$.

2.2.3. 2,6-Dibenzothiazolyl-4-methylphenol (*3*)

2,6-diformyl-4-methylphenol was firstly synthesized according to the reported procedure [35]. Briefly, under N_2 atmosphere, 4-methylphenol (10 mmol) and hexamethylenetetramine (40 mmol) were dissolved in TFA (15 mL) and refluxed at 110 °C for 48 h. The mixture was cooled to room temperature, poured into 4 M HCl solution (80 mL), and extracted with chloroform (3 × 20 mL). The organic layer was combined and washed with 4 M HCl (80 mL), water (80 mL), then dried over $MgSO_4$ and evaporated to dryness under reduced pressure, respectively. The crude product was further purified by column chromatography (silica gel, hexane/ethyl acetate = 20:1 v/v). Yield: 60.9%. ^{1}H NMR (400 MHz, $CDCl_3$), δ (ppm): 11.48 (s, 1H), 10.24 (s, 2H), 7.79 (s, 2H), 2.41 (s, 3H); ^{13}C NMR (100 MHz, $CDCl_3$), δ (ppm): 192.22, 161.77, 137.99, 129.53, 122.92, 20.09. Then **3** was prepared by employing the similar procedure described for **2**. The pure **3** was isolated as pale yellow solid by column chromatography (silica gel, hexane/dichloromethane = 4:1 v/v). Yield: 8%. ^{1}H NMR (400 MHz, $CDCl_3$), δ (ppm): 8.13 (d, J = 8 Hz, 4H), 7.99 (d, J = 8 Hz, 2H), 7.57 (t, J = 8 Hz, 2H), 7.46 (t, J = 8 Hz, 2H), 2.51 (s, 3H); ^{13}C NMR (100 MHz, $CDCl_3$), δ (ppm): 154.25, 151.43, 132.01, 126.56, 125.35, 122.37, 121.51, 29.71, 20.53. MALDI-TOF-MS: *m*/*z* calcd for $C_{21}H_{14}N_2OS_2$, 374.05; found 375.12 $(M + H)^+$. Elemental Anal: calcd for $C_{21}H_{14}N_2OS_2$, C 67.35%, H 3.77%, N 7.48%; found C 67.50%, H 4.63%, N 6.42%.

2.2.4. 2,4,6-Tribenzothiazolylphenol (*4*)

Firstly, 3,5-diformyl-4-hydroxybenzoic acid was synthesized according to the reported procedure [36]. Briefly, under N_2 atmosphere, 4-hydroxybenzoic acid (10 mmol) and hexamethylenetetramine (40 mmol) were dissolved in TFA (15 mL) and refluxed at 110 °C for 72 h. After cooling to room temperature, the mixture was poured into ice water (80 mL), and the product was obtained by filtration. Yield: 55%. ^{1}H NMR (400 MHz, DMSO-d_6), δ (ppm): 13.34 (s, 1H), 10.30 (s, 2H), 8.55 (s, 2H); ^{13}C NMR (100 MHz, DMSO-d_6), δ (ppm): 192.42, 165.99, 165.30, 138.05, 124.07, 123.06. Then **4** was prepared by employing the similar procedure described for **2**. The pure **4** was isolated as pale yellow solid by column chromatography (silica gel, hexane/dichloromethane = 1:1 v/v). Yield: 5.2%. ^{1}H NMR (400 MHz, $CDCl_3$), δ (ppm): 9.16 (s, 2H), 8.20 (t, J = 8 Hz, 3H), 8.03 (d, J = 8 Hz, 2H), 7.99 (d, J = 8 Hz, 1H), 7.61 (m, 3H), 7.51 (m, 3H). MALDI-TOF-MS: *m*/*z* calcd for $C_{27}H_{15}N_3OS_3$, 493.04; found 494.12 $(M + H)^+$. Elemental Anal: calcd for ($C_{27}H_{15}N_3OS_3$ + hexane), C 68.36%, H 5.04%, N 7.25%; found: C 68.10%, H 5.33%, N 6.73%.

2.2.5. 1,3,5-Trisbenzothiazolylbenzene (*5*)

Control compound **5** was synthesized according to the reported procedure [37]. Briefly, under N_2 atmosphere, 1,3,5-

benzenetricarboxylic acid (5 mmol) and 2-aminothiophenol (15 mmol) were dissolved in polyphosphoric acid (8 mL)and heated at 230 °C for 12 h. The mixture was cooled to room temperature, poured into ice water (100 mL), and neutralized with sodium bicarbonate, respectively. The obtained brown solid was recrystallized from chloroform to give **5** as a grey-white solid. Yield: 2.7%. ^{1}H NMR (400 MHz, $CDCl_3$), δ (ppm): 9.02 (s, 3H), 8.24 (d, J = 8 Hz, 3H), 8.01 (d, J = 8 Hz, 3H), 7.60 (t, J = 8 Hz, 3H), 7.50 (t, J = 8 Hz, 3H); ^{13}C NMR (100 MHz, $CDCl_3$), δ (ppm): 166.12, 153.36, 135.12, 135.06, 128.57, 126.85, 125.98, 123.47, 121.88.

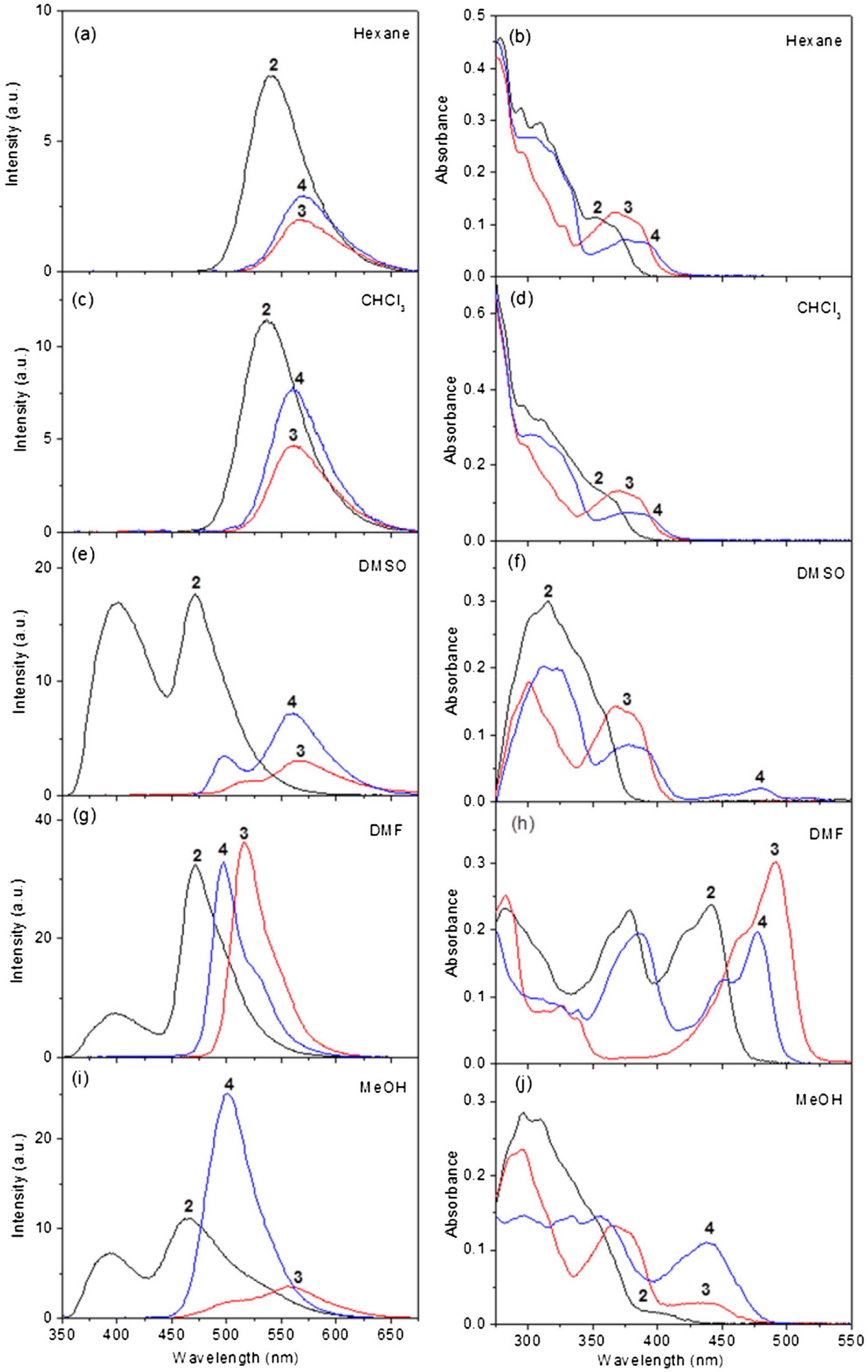

Fig. 2. Absorption (b, d, f, h, j) and fluorescence (a, c, e, g, i) spectra of **2–4** in various solvents. Excitation wavelength is 345 nm.

2.3. DFT calculations

All calculations were performed using Gaussian 09 package [38]. The ground state (S_0) and the first singlet excited state (S_1) geometries of the compounds were optimized in the gas phase using density functional theory (DFT) and time-dependent density functional theory (TDDFT) at the B3LYP/6-31 + G(d) level, respectively. The absorption and fluorescence emission were calculated with TDDFT based on the optimized S_0 and S_1 state geometries, respectively.

Table 1
Photophysical Properties of Compounds 2–4 in various solvents.

Compounds	Solvents	λ_{Abs}[a] (nm)	ε[b] (M^{-1} cm^{-1})	λ_{Flu}[c] (nm)	Φ_F[d]
2	Hexane	356	11,240	541	0.051
	$CHCl_3$	360	12,330	537	0.066
	DMSO	316	29,980	401/472	0.301
	DMF	378/441	22,960/23,430	397/472	0.212
	MeOH	303/400	27,320/1570	393/466	0.122
3	Hexane	369	12,420	568	0.029
	$CHCl_3$	370	12,996	560	0.086
	DMSO	301/375	17,820/13,650	518/566	0.066
	DMF	325/491	8676/30,250	516	0.381
	MeOH	295/372/439	23,090/13,030/3012	560	0.069
4	Hexane	378	7172	570	0.047
	$CHCl_3$	380	7562	560	0.056
	DMSO	318/382/480	20,480/8510/2160	497/560	0.068
	DMF	387/477	19,510/19,650	497	0.162
	MeOH	440	10,980	502	0.302

[a] The maximum absorption wavelength.
[b] The molar absorption coefficient.
[c] The maximum fluorescence emission wavelength (λ_{ex} = 345 nm).
[d] The fluorescence quantum yield measured by using quinine sulfate ($\Phi_f = 0.546$) as a standard.

3. Results and discussion

3.1. Absorption and fluorescence spectra

The absorption and fluorescence spectra of HBT derivatives **1–4** were studied in hexane, $CHCl_3$, DMSO, DMF and MeOH (Fig. 2 and Figure S1). As shown in Figure 2, **4** exhibits a solvent-dependent absorption and emission behavior. In nonpolar solvents hexane and $CHCl_3$, **4** shows an absorption band at 350–450 nm, accompanied by shoulders around 290–350 nm (Fig. 2b and d), respectively. The low energy absorption band are due to the S_0–S_1 ($\pi\pi^*$) transition, which is assigned to the intramolecular hydrogen-bonding closed enol conformer (E–E*, Scheme 1, vide infra DFT calculation section). **2** and **3** present similar absorption behaviors in these solvents, but their wavelengths of low energy absorption bands are slightly short than that of **4** (Fig. 2 and Table 1), implying a larger conjugation in tri-HBT **4**. In polar solvents DMSO, DMF and MeOH, a new low energy absorption band appeared around 400–500 nm for **4** (Fig. 2f, h and j), which can be attributed to the deprotonated anion conformer (A–A*, Scheme 1, vide infra F titration section) due to the solvent-assisted deprotonation interaction. In contrast, the absorption spectra of HBT **1** only showed a slight change with variation of solvents (Figure S1), suggesting the presence of a weak influence of inter- and intramolecular hydrogen bonding on the absorption spectra.

On the other hand, **4** shows a single emission band at about 500–650 nm in nonpolar solvents hexane and $CHCl_3$ with a large stokes-shift of ca. 9000 cm^{-1} (Fig. 2a and c), which is a typical characteristic of ESIPT emission from keto tautomer (K*–K, Scheme 1). As shown in Scheme 1, the K* state was derived from E* state via an ESIPT process, relaxed to ground state (K) through ESIPT emission and followed by back ground state intramolecular proton transfer (GSIPT) to the more stable ground state enol

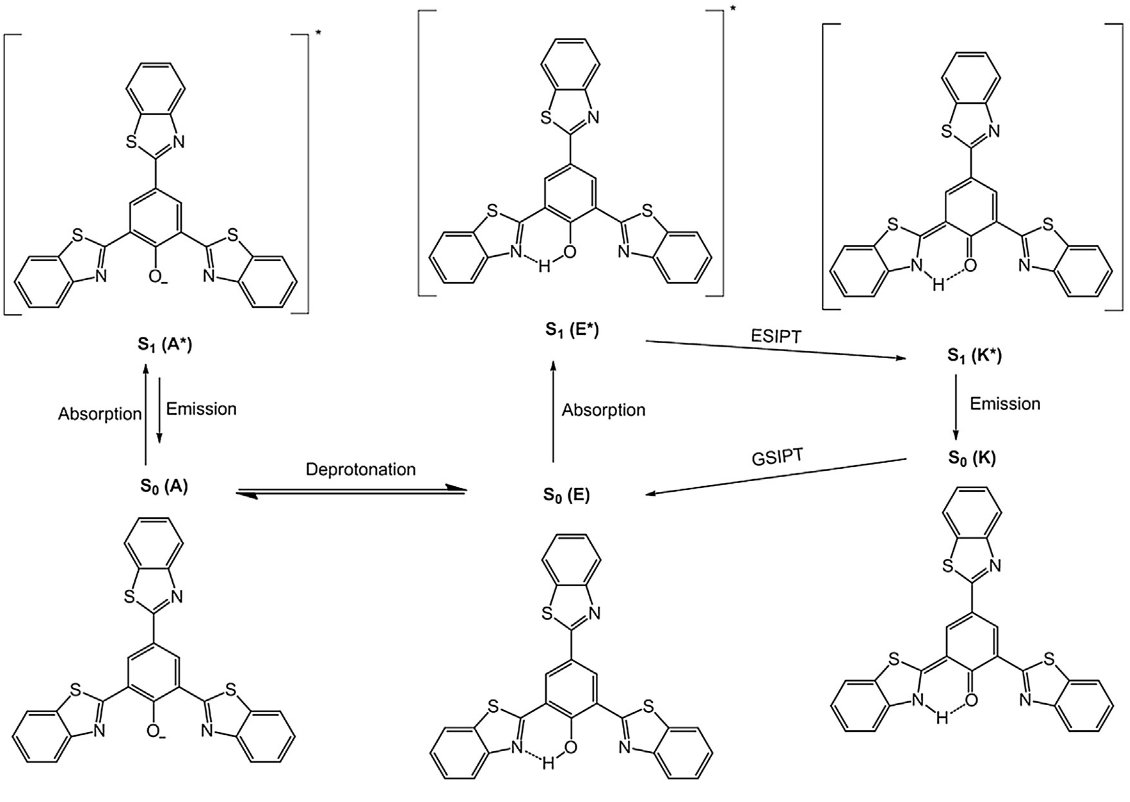

Scheme 1. Schematic representation of the photophysical processes for **4**.

tautomer [13,26]. Such long ESIPT emission was also observed in **1**–**3** derivatives, respectively (Fig. 2a, b and S1, Table 1). In DMSO, **4** gives a dual emission, where a new weak emission appeared around 500 nm, ascribed to the deprotonated anion conformer (A*–A, Scheme 1), besides the longer keto tautomer emission around 565 nm (Fig. 2e). And in DMF and MeOH, **4** only gives a strong emission from the deprotonated anion conformer (A*–A, Scheme 1) with the maximum wavelength of 500 nm (Fig. 2g and i), which is in well agreement with anion bands observed in the absorption spectra (Fig. 2h and j). While **3** exhibits the similar emission behavior with that **4**, both **1** and **2** show a different dual fluorescence, where two new emissions appeared around 400 nm and 475 nm in these polar solvents (Fig. 2e, g and i and S1), ascribed to the neutral enol and anion conformers, respectively [28,32].

The excitation spectra of **1**–**4** recorded in different solvents resemble their corresponding absorption spectra (Figure S2), revealing that the fluorescence emission originates from the ground state absorbing species. The fluorescence emission and quantum yields of HBT derivatives **1**–**4** in different solvents are summarized in Table 1. The absence of enol emission for **3** and **4** in these solvents suggests that their enol forms in the excited state are not stable, probably resulted from their two symmetric benzothiazole moieties of proximity to phenolic OH that makes the closed H-bonding conformer predominant. In contrast, strong enol emission was observed for **1** and **2** in polar solvents due to the intramolecular hydrogen bond between phenolic OH and N atom of benzothiazole moiety is disrupted by solvent molecule, made an open form conformer predominant [26,28]. The control compound **5** that could not undergo ESIPT due to the absence of phenolic OH, showed a near solvent-independent absorption and fluorescence spectra (Figure S3), indicating that the phenolic OH is crucial in **4** for its solvent-dependent photophysical properties.

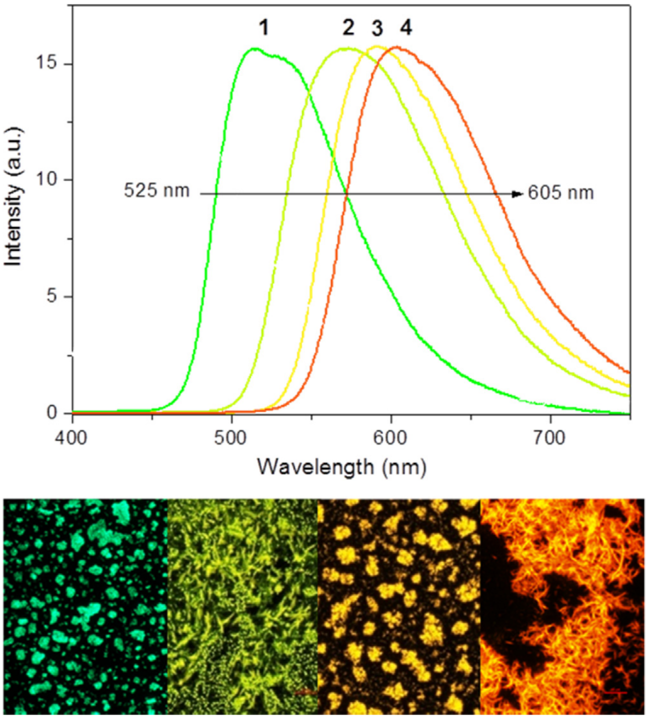

Fig. 4. Solid state fluorescence spectra of **1**–**4** (up) and their corresponding fluorescence microscopic images (bottom). Excitation wavelength is 345 nm.

3.2. White emission and solid state fluorescence

The solvent-dependent multiple emission from blue to green, yellow and red of HBT derivatives **1**–**4** covers a broad visible region, making it promising to be utilized for developing color tunable fluorescence even white by simply mixing them together [39]. For example, in DMSO, **4** gives two emission bands located around 500 nm and 600 nm, whereas **2** presents dual emission around 400 nm and 500 nm, and color tunable fluorescence from blue to yellow was obtained by gradually mixing **2** with **4**. More interestingly, a white emission was successfully created at a ratio of 0.5, where three emission bands around 400 nm, 500 nm and 600 nm appear at the same time (Fig. 3a). The CIE chromaticity diagram (Fig. 3b) clearly shows the fluorescence color change with the ratio of **2** and **4**, where near pure white coordinates (0.33, 0.33) were obtained at **2**/**4** ratios of 1:1 (0.33, 0.34) and 4:3 (0.31, 0.32), respectively.

The solid state fluorescence of **4** was investigated by measuring powder samples. As shown in Fig. 4, a NIR emission with the maximum around 605 nm and a fluorescence quantum yield of 30% was observed in **4**, whereas the corresponding value is 525 nm (60%), 575 nm (40%) and 592 nm (40%) in **1**–**3**, respectively. The fluorescence microscopic images clearly demonstrated the solid state emission color change from green to yellow and red of **1**–**4** (Fig. 4). This reveals that the extending of π-conjugation could create the red emitting HBT derivatives, which will contribute to develop highly emissive NIR fluorescent materials based on the ESIPT chromophores [40].

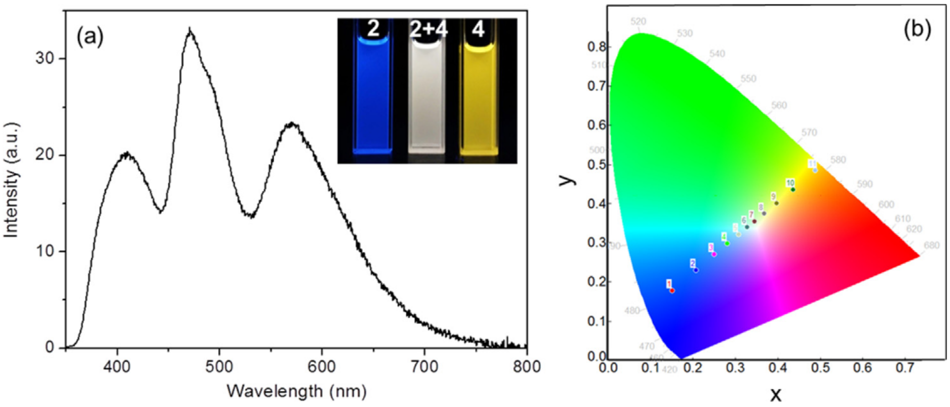

Fig. 3. Fluorescence spectrum ($\lambda_{ex} = 345$ nm) of the mixture of **2** and **4** at a ratio of 1:1 in DMSO (a), and CIE chromaticity diagram of the mixture of **2** and **4** at various ratios, where the ratio of **2**/**4** changed from 10:0 to 0:10 from dot 1 to 11 (b). Inset in (a) is photographs of **2**, 1:1 mixture of **2** + **4** and **4** in DMSO under a UV lamp (365 nm) irradiation.

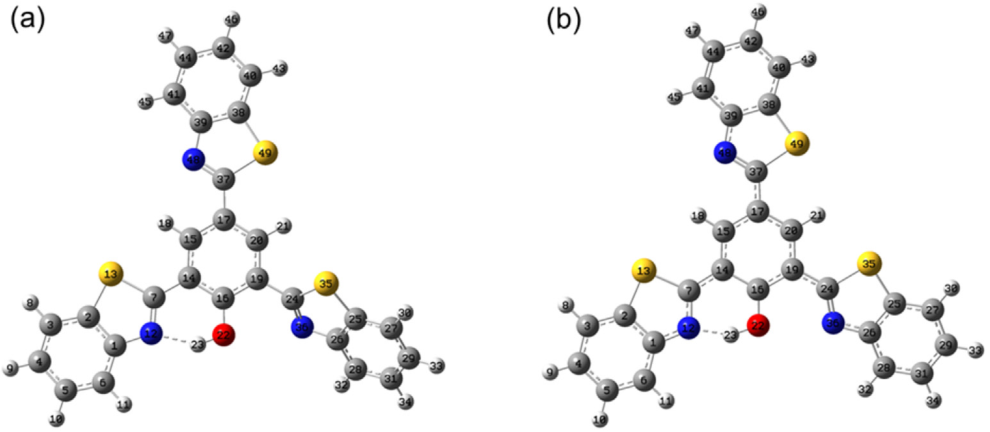

Fig. 5. Optimized molecular structure of **4** in S_0 (a) and S_1 (b) states.

3.3. DFT calculations

To further investigate the photophysical property of tri-HBT derivative **4**, DFT/TDDFT calculations have been performed in the gas phase. The ground and exited state geometries of the HBT derivatives were optimized with DFT and TDDFT methods at the B3LYP/6-31 + G(d) level, respectively. The UV–vis absorption and the fluorescence emission of the compounds were calculated with TDDFT methods based on optimized S_0 and S_1 state geometries, respectively.

The optimized S_0 and S_1 state geometries of **4** are shown in Fig. 5. In the ground state, two benzothiazole moieties (2 and 4 position) are near coplanar with phenol ring, but the third benzothiazole unit (6-position) is twisted about 45° from phenol plane (Fig. 5). The twisting of the non-hydrogen bonded benzothiazole from the phenol ring could rationalized by considering the phenolic OH steric hindrance, which is supported by the planar molecular geometry of the control compound **5** optimized at the same calculation method. Upon excitation, the dihedral angle between the twisted benzothiazole moiety (6-position) and phenol ring is around 15°, indicating a structural reorganization occurs and the molecule becomes more planar at the S_1 state (Fig. 5). Regarding to the structural parameters involved in the hydrogen bond, it is noted that the bond length of O–H elongated from 0.9963 Å (in S_0) to 1.0493 Å (in S_1), the distance of N···H became shorter from 1.7356 Å (in S_0) to 1.5398 Å (in S_1), and the angle of O–H···N enlarged from 146.82° (in S_0) to 152.02° (in S_1). These structural changes indicate that the intramolecular hydrogen bond (O–H···N) is substantially strengthened in the S_1 state, facilitating the occurrence of ESIPT [41]. The calculated absorption and emission maximum wavelength of **4** are 383.78 nm and 618.85 nm, respectively, which are close to the experimental results (376 nm and 570 nm in hexane, Fig. 2). By comparison with others HBT derivatives **1**–**3**, it is noted that both the absorption and emission maximum undergo red-shift with extending the π-conjugation (Table S1). The frontier molecular orbitals of **1–4** were further calculated and the highest occupied molecular orbital (HOMO) and the lowest unoccupied molecular orbital (LUMO) are depicted in Fig. 6. Notably, the HOMO delocalized on whole molecule and the LUMO mainly distributed on hydrogen bonding involved HBT moiety (Fig. 6), suggesting a predominant π–π* transition character of E–E* (Scheme 1).

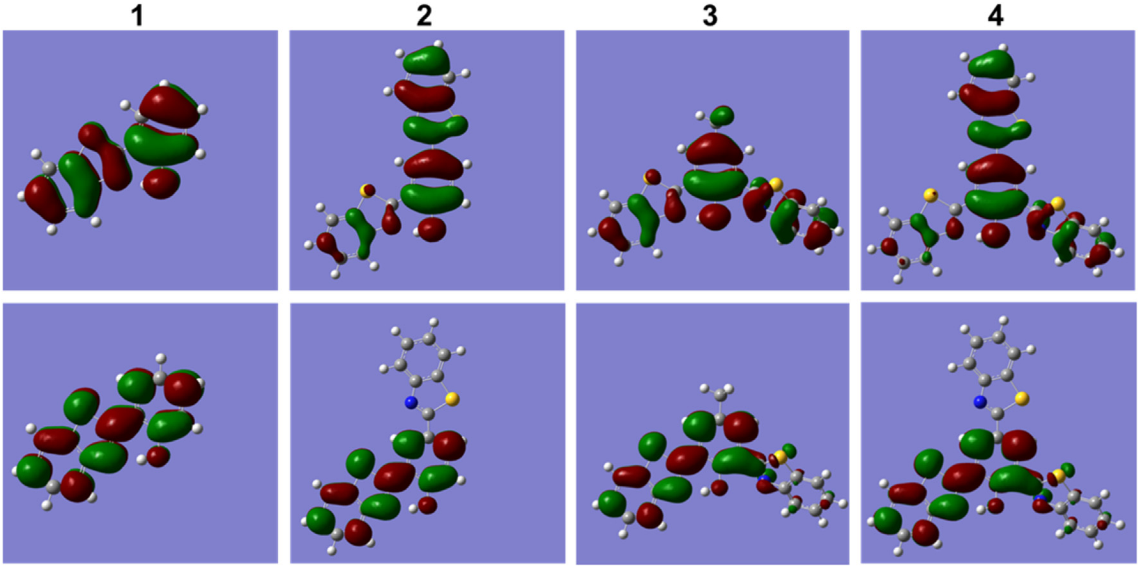

Fig. 6. HOMO (up) and LUMO (bottom) orbitals of **1–4** in the ground state.

3.4. *Ratiometric fluorescence sensing of anions*

The solvent dependent multiple emission of **4** makes it promising to be utilized for developing ratiometric fluorescent probes [20,42,43]. Therefore, the sensing property for anions such as fluoride (F^-) was investigated in DMSO. As shown in Fig. 7, all HBT derivatives showed a ratiometric fluorescence response toward F^-.

For example, without F^- addition, **4** shows dual fluorescence, originating from both keto conformer (K*–K, Scheme 1) and anion (A*–A, Scheme 1) respectively; upon introduction of F^-, the keto emission (560 nm) decreased and anion emission (500 nm) increased with an iso-emissive point at 550 nm (Fig. 7g). At the same time, the absorption spectra also showed an obvious change upon addition of F^-, where the anion absorption band around 475 nm enhanced and the absorption band around 300 nm decreased with an isobestic point at 345 nm (Fig. 7h), indicating the F^--induced a ground state deprotonation of phenolic OH in **4** [44–46]. Similarly, the F^--induced enhancements of anion emission and absorption were also observed in others HBT derivatives **1**–**3** (Fig. 7a–f). However, both the absorption and fluorescence spectra of control compound **5** did not show any noticeable change with addition of F^-, further confirming that the phenolic OH is crucial in **4** for ratiometric fluorescence sensing property toward F^-. It should be noted that the emitting species involved in **3** and **4** are keto conformer and anion, whereas in **1** and **2**, enol conformer and anion. Furthermore, **4** showed the highest sensitivity toward F^- sensing, where the fluorescence response observed even 5 equiv F^- addition and reaches the maximum upon 40 equiv F^- addition, but others derivatives **1**–**3** only showed the obvious response upon more than 40 equiv F^- addition (Fig. 7). The difference on the

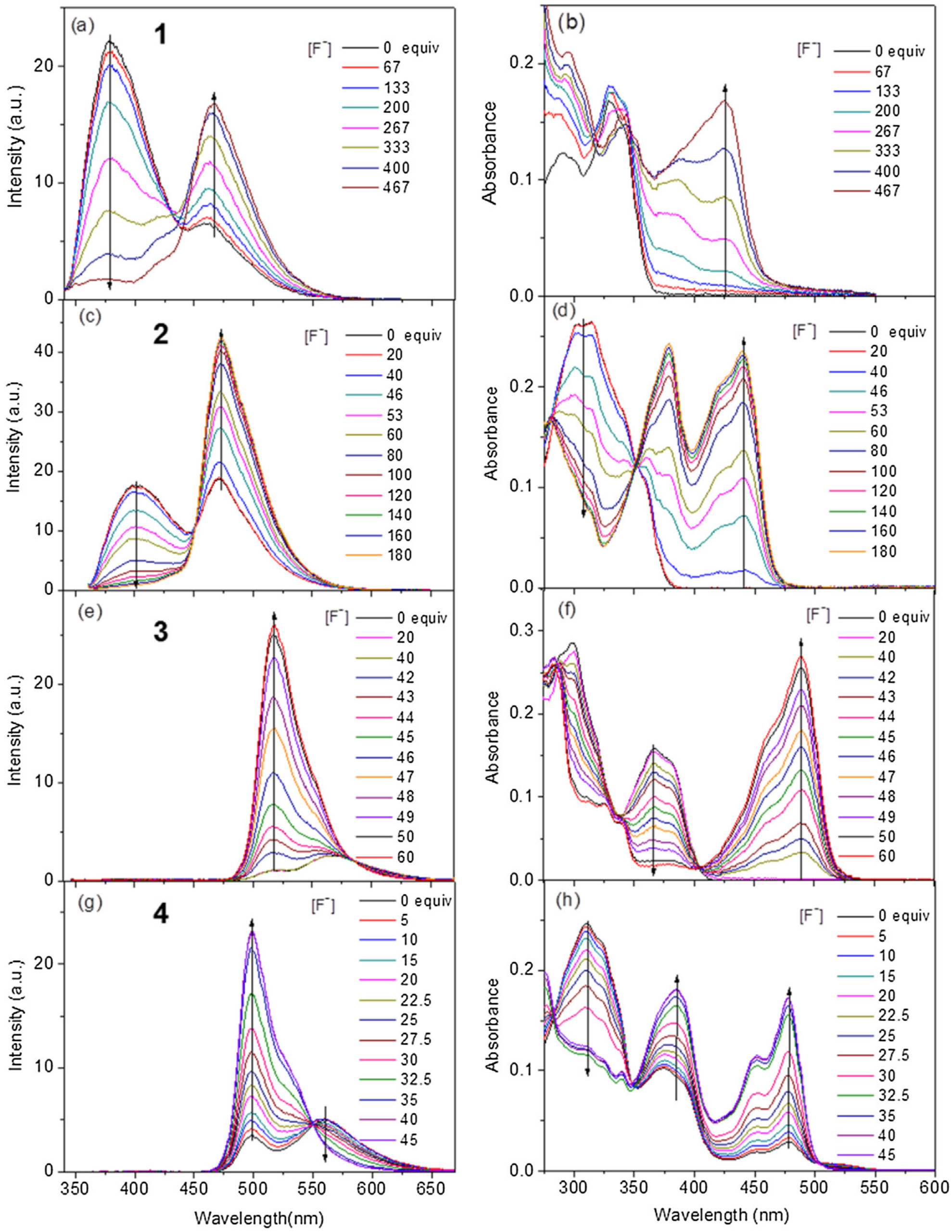

Fig. 7. Change of fluorescence (a, c, e, g) and absorption (b, d, f, h) spectra of **1–4** (10 μM) in DMSO with addition of various amounts of F^-.

sensitivity reveals that the anion sensing property could be tuned by proper modification of molecular structure. These results may contribute to develop the ratiometric fluorescent probes based on the ESIPT chromophores.

4. Conclusions

In summary, 2,4,6-trisbenzothiazolylphenol (**4**) was prepared as a new excited state intramolecular proton transfer (ESIPT) chromophore. The photophysical properties were studied with absorption and emission spectroscopies as well as theoretical calculations. It was found that **4** showed solvent dependent absorption and fluorescence emission. In the nonpolar solvents (hexane etc.), ESIPT occurred and only keto tautomer emission at 570 nm was observed, whereas an emission at 510 nm from the deprotonated anion species was observed in polar solvents (DMF etc.). With addition of fluoride into DMSO solution of **4**, the keto emission was quenched, whereas the emission from anion form was drastically enhanced, making a ratiometric fluorescence sensing of fluoride achievable. In solid state, **4** showed a near-infrared (NIR) ESIPT fluorescence emission at 605 nm, which is longer than those of parent molecule 2-(2-hydroxyphenyl)benzothiazole (HBT, **1**) (525 nm), 2,4-dibenzothiazolylphenol (**2**, 575 nm) and 4-methyl-2,6-dibenzothiazolylphenol (**3**, 592 nm) respectively. Thus, the color tuning of solid state ESIPT emission of the HBT chromophore was achieved from green to yellow and near-infrared by properly extending the π-conjugation that was further confirmed by TDDFT calculations. The white emission was also created by simply mixing two HBT derivatives in DMSO. These investigations will be useful for designing new ESIPT chromophore and developing ESIPT-based highly emissive NIR fluorescent materials and ratiometric fluorescent probes.

Acknowledgment

This work was financially supported by the Research Fund for the Doctoral Program of Higher Education of China (No. 20120075120018), Fundamental Research Funds for the Central Universities (Nos. 2232014D3-11, 2232015G1-61), and the National Natural Science Foundation of China (No. 51203018).

Appendix A. Supplementary data

Supplementary data related to this article can be found at http://dx.doi.org/10.1016/j.dyepig.2015.10.002.

References

[1] Arnaut LG, Formosinho SJ. Excited-state proton transfer reactions I. Fundamentals and intermolecular reactions. J Photochem Photobiol A 1993;75:1–20.

[2] Formosinho SJ, Arnaut LG. Excited-state proton transfer reactions II. Intramolecular reactions. J Photochem Photobiol, A 1993;75:21–48.

[3] Zhao J, Ji S, Chen Y, Guo H, Yang P. Excited state intramolecular proton transfer (ESIPT): from principal photophysics to the development of new chromophores and applications in fluorescent molecular probes and luminescent materials. Phys Chem Chem Phys 2012;14:8803–17.

[4] Hsieh C-C, Jiang C-M, Chou P-T. Recent experimental advances on excited-state intramolecular proton coupled electron transfer reaction. Acc Chem Res 2010;43:1364–74.

[5] Kwon JE, Park SY. Advanced organic optoelectronic materials: harnessing excited-state intramolecular proton transfer (ESIPT) process. Adv Mater 2011;23:3615–42.

[6] Park S, Kwon JE, Park SY. Strategic emission color tuning of highly fluorescent imidazole-based excited-state intramolecular proton transfer molecules. Phys Chem Chem Phys 2012;14:8878–84.

[7] Sun W, Li S, Hu R, Qian Y, Wang S, Yang G. Understanding solvent effects on luminescent properties of a triple fluorescent ESIPT compound and application for White light emission. J Phys Chem A 2009;113:5888–95.

[8] Demchenko AP, Tang K-C, Chou P-T. Excited-state proton coupled charge transfer modulated by molecular structure and media polarization. Chem Soc Rev 2013;42:1379–408.

[9] Kim CH, Park J, Seo J, Park SY, Joo TJ. Excited state intramolecular proton transfer and charge transfer dynamics of a 2-(2-Hydroxyphenyl)benzoxazole derivative in solution. J Phys Chem A 2010;114:5618–29.

[10] Chuang W, Hsieh C, Lai C, Lai C, Shih C, Chen K, et al. Excited-state intramolecular proton transfer molecules bearing o-hydroxy analogues of green fluorescent protein chromophore. J Org Chem 2011;76:8189–202.

[11] Lim S-J, Seo J, Park SY. Photochromic switching of excited-state intramolecular proton-transfer (ESIPT) fluorescence: a unique route to high-contrast memory switching and nondestructive readout. J Am Chem Soc 2006;128:14542–7.

[12] Houari Y, Chibani S, Jacquemin D, Laurent D. Td-dft assessment of the excited state intramolecular proton transfer in hydroxyphenylbenzimidazole (HBI) dyes. J Phys Chem B 2015;119:2180–92.

[13] Majumdar P, Zhao J. 2-(2-hydroxyphenyl)-benzothiazole (HBT)-rhodamine dyad: acid-switchable absorption and fluorescence of excited-state intramolecular proton transfer (ESIPT). J Phys Chem B 2015;119:2384–94.

[14] Tomin VI, Demchenko AP, Chou P-T. Thermodynamic vs. kinetic control of excited-state proton transfer reactions. J Photochem Photobiol C 2015;22:1–18.

[15] Zhang X, Guo L, Wu F-Y, Jiang Y-B. Development of fluorescent sensing of anions under excited-state intermolecular proton transfer signaling mechanism. Org Lett 2003;15:2667–70.

[16] Wu Y, Peng X, Fan J, Gao S, Tian M, Zhao J, et al. Fluorescence sensing of anions based on inhibition of excited-state intramolecular proton transfer. J Org Chem 2007;72:62–70.

[17] Xu Y, Pang Y. Zinc binding-induced near-IR emission from excited-state intramolecular proton transfer of a Bis(benzoxazole) derivative. Chem Commun 2010;46:4070–2.

[18] Murale DP, Kim H, Choi WS, Churchill DG. Highly selective excited state intramolecular proton transfer (ESIPT)-based superoxide probing. Org Lett 2013;15:3946–9.

[19] Chen H, Lin W, Cui H, Jiang W. Development of unique xanthene–cyanine fused near-infrared fluorescent fluorophores with superior chemical sability for biological fluorescence imaging. Chem Eur J 2015;21:733–45.

[20] Geng L, Yang X-F, Zhong Y, Li Z, Li H. "Quinoneephenol" transduction activated excited-state intramolecular proton transfer: a new strategy toward ratiometric fluorescent probe for sulfite in living cells. Dyes Pigm 2015;120:213–9.

[21] Goodman J, Brus LE. Proton transfer and tautomerism in an excited state of methyl salicylate. J Am Chem Soc 1978;100:7472–4.

[22] Zhou P, Hoffmann MR, Han K, He G. New insights into the dual fluorescence of methyl salicylate: effects of intermolecular hydrogen bonding and solvation. J Phys Chem B 2015;119:2125–31.

[23] Klymchenko AS, Demchenko AP. Electrochromic modulation of excited-state intramolecular proton transfer: the new principle in design of fluorescence sensors. J Am Chem Soc 2002;124:12372–9.

[24] Ghosh D, Batuta S, Das S, Begum NA, Mandal D. Proton transfer dynamics of 4′-*N*,*N*-Dimethylamino-3-hydroxyflavone observed in hydrogen-bonding solvents and aqueous micelles. J Phys Chem B 2015;119:5650–61.

[25] Abou-Zied OK, Jimenez R, Thompson EHZ, Millar DP, Romesberg FE. Solvent-dependent photoinduced tautomerization of 2-(2′-Hydroxyphenyl)benzoxazole. J Phys Chem A 2002;106:3665–72.

[26] Yuan Z, Tang Q, Sreenath K, Simmons JT, Younes AH, Jiang D, et al. Absorption and emission sensitivity of 2-(2'-Hydroxyphenyl)benzoxazoleto solvents and impurities. Photochem Photobiol 2015;91:586–98.

[27] Mohammed OF, Luber S, Batista VS, Nibbering ETJ. Ultrafast branching of reaction pathways in 2-(2′-Hydroxyphenyl)benzothiazole in polar acetonitrile solution. J Phys Chem A 2011;115:7550–8.

[28] Aly SM, Usman A, AlZayer A, Hamdi GA, Alarousu E, Mohammed OF. Solvent-dependent excited-state hydrogen transfer and intersystem crossing in 2-(2′-Hydroxyphenyl)-Benzothiazole. J Phys Chem B 2015;119:2596–603.

[29] Cheng J, Liu D, Bao J, Xu K, Yang Y, Han K. A single 2-(2'-Hydroxyphenyl) benzothiazole derivative can achieve pure white-light emission. Chem Asian J 2014;9:3215–20.

[30] Yao D, Zhao S, Guo J, Zhang Z, Zhang H, Liu Y, et al. Hydroxyphenyl-benzothiazole based full color organic emitting materials generated by facile molecular modification. J Mater Chem 2011;21:3568–70.

[31] Luo W, Jiang H, Zhang K, Liu W, Tang X, Dou W, et al. A reusable ratiometric two-photon chemodosimeter for Hg^{2+} detection based on ESIPT and its application in bioimaging. J Mater Chem B 2015;3:3459–64.

[32] Sakai K-I, Ishikawa T, Akutagawa T. A blue-White-yellow color-tunable excited state intramolecular proton transfer (ESIPT) fluorophore: sensitivity to polar–nonpolar solvent ratios. J Mater Chem C 2013;1:7866–71.

[33] Melhuish WH. Quantum efficiencies of fluorescence of organic substances: effect of solvent and concentration of the fluorescent solute. J Phys Chem 1961;65:229–35.

[34] Jena B, Manoharan SS, Prakash S. Specificity and selectivity in photoluminescent properties of π-conjugated benzheterazole molecules. J Phys Chem C 2009;113:20942–8.

[35] Chen X, Wang J, Sun S, Fan J, Wu S, Liu J, et al. Efficient enhancement of DNA cleavage activity by introducing guanidinium groups into Diiron(III) complex. Bioorg Med Chem Lett 2008;18:109–13.

[36] Karton-Lifshin N, Albertazzi L, Bendikov M, Baran PS, Shabat D. "Donor–two-acceptor" dye design: a distinct gateway to NIR fluorescence. J Am Chem Soc 2012;134:20412–20.

[37] Chandrashekhar N, Thomas B, Gayathri V, Ramanathan KV, Gowda NMN. Synthesis and NMR spectral assignments of novel nitrogen and sulfur heterocyclic compounds. Magn Reson Chem 2008;46:769–74.
[38] Frisch MJ, Trucks GW, Schlegel HB, Scuseria GE, Robb MA, Cheeseman JR, et al. Gaussian 09, Revision C.01. Wallingford, CT: Gaussian Inc.; 2010.
[39] Mukherjee S, Thilagar P. Organic white-light emitting materials. Dyes Pigm 2014;110:2–27.
[40] Sakai K-I, Kawamura H, Kobayashi N, Ishikawa T, Ikeda C, Kikuchi T, et al. Highly efficient solid-state red fluorophores using ESIPT: crystal packing and fluorescence properties of alkoxy-substituted dibenzothiazolylphenols. Cryst Eng Comm 2014;16:3180–5.
[41] Zhao J, Chen J, Liu J, Hoffmann MR. Competitive excited-state single or double proton transfer mechanisms for bis-2,5-(2-benzoxazolyl)-hydroquinone and its derivatives. Phys Chem Chem Phys 2015;17:11990–9.
[42] Goswami S, Manna A, Paul S, Das AK, Aich K, Nandi PK. Resonance-assisted hydrogen bonding induced nucleophilic addition to hamper ESIPT: ratiometric detection of cyanide in aqueous Media. Chem Commun 2013;49:2912–4.
[43] Lee MH, Kim JS, Sessler JL. Small molecule-based ratiometric fluorescence probes for cations, anions, and biomolecules. Chem Soc Rev 2015;44:4185–91.
[44] Peng X, Wu Y, Fan J, Tian M, Han K. Colorimetric and ratiometric fluorescence sensing of fluoride: tuning selectivity in proton transfer. J Org Chem 2005;70:10524–31.
[45] Zhang X, Shiraishi Y, Hirai T. Unmodified fluorescein as a fluorescent chemosensor for fluoride ion detection. Tetrahedron Lett 2007;48:8803–6.
[46] Martínez-Máñez R, Sancenón F. Fluorogenic and chromogenic chemosensors and reagents for anions. Chem Rev 2003;103:4419–76.